REAL-TIME MAGNETIC ELECTRON ENERGY SPECTROMETER FOR USE WITH MEDICAL LINEAR ACCELERATORS

P. E. Maggi[†], K. R. Hogstrom, K. L. Matthews II,
Louisiana State University, Baton Rouge, LA 70803, USA
R. L. Carver, Mary Bird Perkins Cancer Center, Baton Rouge, LA 70809, USA

Abstract

Accelerator characterization and quality assurance is an integral part of electron linear accelerator (linac) use in a medical setting. The current clinical method for radiation metrology of electron beams (dose on central axis versus depth in water) only provides a surrogate for the underlying performance of the accelerator and does not provide direct information about the electron energy spectrum. We have developed an easy to use real-time magnetic electron energy spectrometer for characterizing the electron beams of medical linacs. Our spectrometer uses a 0.57 T permanent magnet block as the dispersive element and scintillating fibers coupled to a CCD camera as the position sensitive detector. The goal is to have a device capable of 0.12 MeV energy resolution (which corresponds to a range shift of 0.5 mm) with a minimum readout rate of 1 Hz, over an energy range of 5 to 25 MeV. This work describes the real-time spectrometer system, the detector response model, and the spectrum unfolding method. Measured energy spectra from multiple electron beams from an Elekta Infinity Linac are presented.

INTRODUCTION

Many cancer centers have multiple medical linear accelerators (linacs) used for treating patients. The linacs produce beams of photons or electrons; typical electron energies range from 4 MeV to 25 MeV. If all of the linacs at a cancer center have matched beams, which include matched dose vs depth curves, patients can be treated with any machine at the facility without the need to recalculate machine specific treatment plans. This is especially beneficial if a treatment machine is out of operation, as the patient can easily and immediately be treated on another machine.

The depth-dose curve of a therapeutic electron beam strongly depends on the energy distribution of the incident beam, primarily the mean energy and most probable energy [1]. Depth-dose curves are typically measured using a large water tank with a small diode or ion chamber that is positioned at different depths in the tank. The depth-dose curve reflects only specific features of an energy spectrum, such as peak mean energy (Ep), average energy, and FWHM, but not the spectrum as a whole. Efforts have been made to analytically back calculate the energy spectra from this data [2] or via matching of depth-dose curves with iterative Monte Carlo simulations [3]. These predicted spectra are generated assuming only a Gaussian spectrum that is not excessively broad (e.g. less than 15% FWHM). However it is widely understood

that there is a low-energy tail present in the spectrum [1] as a result of beam conditioning for therapeutic use. Additionally, measurements by Kok et al [4] have shown that spectra for certain traveling-wave linacs (Elekta, Phillips) can have further spectral deviations violating the Gaussian assumption; this is due to accelerator tuning parameters (e.g. High Powered Phase Shifter) relating to the RF recycling system. A magnetic spectrometer has the potential to simplify beam measurements, reduce the time needed for beam matching, and provides more information about the electron beam.

SPECTROMETER HARDWARE

We have developed an easy to use real-time magnetic electron energy spectrometer for characterizing the electron beams of medical linacs. Our spectrometer system is constructed around a 0.57 T (effective field strength) dipole magnet block as the dispersive element; this magnet block was used by McLaughlin et al [5] as part of a passive spectrometer system. The magnet poles measure 15.23 cm x 46.99 cm x 2.63 cm, with a 2.54 cm separation (Fig. 1), and are held apart by steel and aluminium plates. The electron beam enters the magnet block via a 6.35 mm diameter aperture in the steel mounting face. The electrons exit the magnet block at the detector plane, which is the face parallel to both the central axis of the incident electron beam and the direction of the magnetic field.
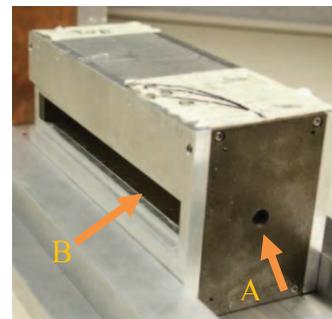

Figure 1: Photograph of magnet block showing the entrance aperture (A) and exit window (B).

The detector system uses a row of 60 1 mm x 1 mm square BCF-20 green scintillating fibers (Saint-Gobain, Malvern, PA) oriented vertically; this provides a one-dimensional position sensitive detector. The fiber ribbon is rearranged to a square bundle to be imaged by a Pixelink PL-8955 monochromatic CCD camera (Fig 2). This design was initially proposed by Gahn et al. [6] for use in high intensity laser plasma studies.
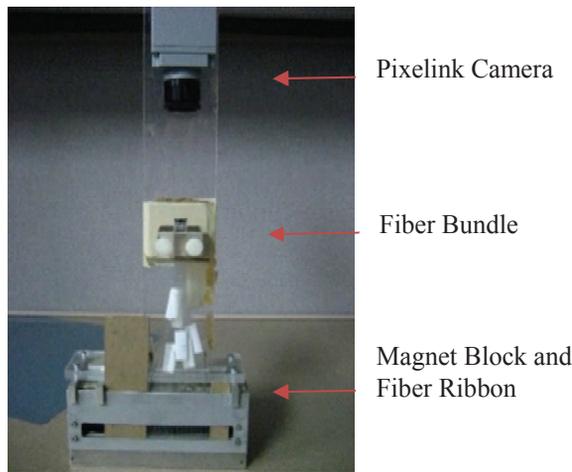
† pmaggi1@lsu.edu

Figure 2: Magnet Block and Fiber Detector System.

To acquire data, the spectrometer is placed on the patient treatment couch with the linac gantry rotated 90^0 (Fig. 3). The broad electron field produced by the accelerator is collimated to a pinhole (diameter 6.35 mm) by a Cerrobend insert at the end of the 10 cm x 10 cm applicator, and is aligned with the entrance to the magnet block.
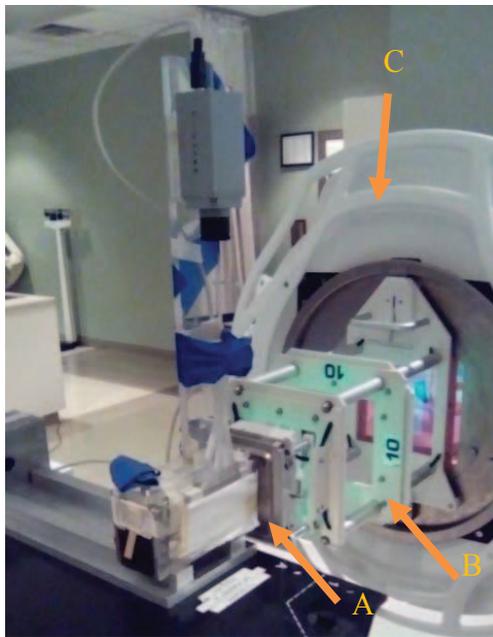

Figure 3: Irradiation Geometry. A is the Cerrobend insert, B is the electron applicator, C is the linac gantry.

The camera acquires images of the fiber bundle (Fig. 4) with an exposure time of 1000 ms. These settings allow for adequate signal accumulation while still providing a frame rate of 1 Hz.

This fiber bundle image is parsed and processed by the analysis software described below.

ANALYSIS SOFTWARE

Fiber response corrections were determined using a 3 cm x 8 cm uniform electron beam directly incident

perpendicular to the long axis of the fiber ribbon. A median filter was used to remove salt and pepper noise.
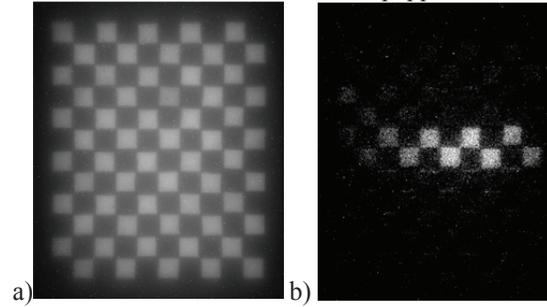

Figure 4: a) Image of fiber bundle during uniform irradiation by a 20 MeV electron beam, used to obtain fiber response correction factors. b) 13 MeV electron beam after background subtraction.

After subtracting a background image (acquired using a solid Cerrobend insert instead of the insert with a pinhole) the fiber signal was summed over the active area of each fiber. This data was sorted into a fiber signal vs position graph as shown in Fig. 5. We used sinc interpolation and a low pass filter to upsample the data and reduce noise.
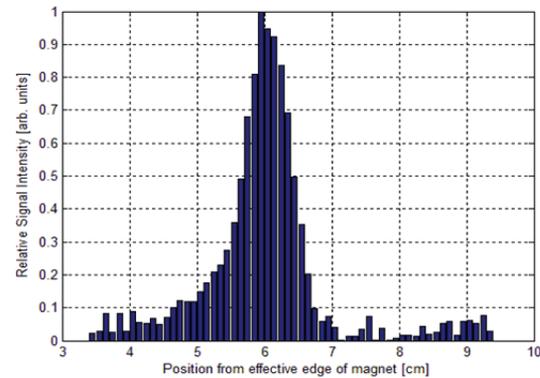

Figure 5: Sorted and corrected fiber signal for a 13 MeV electron beam.

The detector response function (converting from input energy spectrum to output fiber signal) was determined using an in-house Monte Carlo simulation to generate a contribution matrix C. This matrix accounted for the initial Gaussian angular spread of electrons entering the spectrometer through the 6.35 mm aperture, and the finite sized detector elements. In-air scatter was not modelled. The constant magnetic field of 0.57 T was determined using the average field strength experienced by electrons, of energies 3 to 25 MeV, passing through the spectrometer. The contribution matrix allowed the spectrometer to be modelled as a simple linear matrix equation

$$CE = S \qquad (1)$$

where C is the contribution matrix, E is the desired energy spectrum, and S is the resulting fiber signal output. C is not directly invertible, so a basic gradient descent loop, as shown in Eq 2, was used to unfold the data.

$$E_{k+1} = E_k - \omega C^*(CE_k - S) \qquad (2)$$

where E_k is the estimated energy spectrum at the kth iteration, ω is a relaxation factor determined by the largest

singular value of C, and S is the measured fiber signal to be matched. The initial estimate of E_0 was determined by performing a position to energy conversion [5], based on the Lorentz force law, on the sinc interpolated fiber signal assuming a point-like parallel pencil beam input at the center of the aperture.

For sample input data with added noise, this method converged within approximately 200 iterations. However, target real-time operation of 1 Hz will limit the analysis to approximately 50 iterations, which still gives acceptable agreement as shown in Fig. 6 and Table 1. 50 iterations were sufficient to achieve agreement in peak mean energy to within 0.1 MeV and in FWHM to 0.3 MeV.

Table 1: Summary of Fitting Accuracy

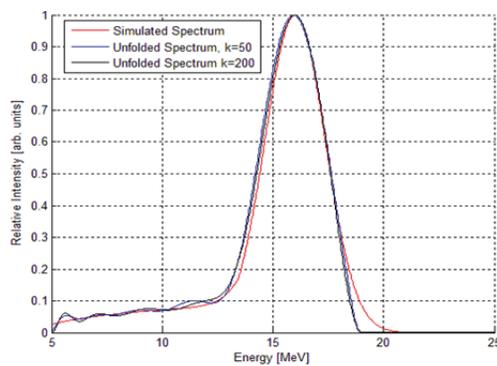|	Peak Mean Energy Ep [MeV]	FWHM [MeV]
Simulated Ideal	16.00	3.20
k = 50	15.93	3.46
k = 200	15.98	3.36

Figure 6: Spectral unfolding at varied number of iterations using simulated data.

ACQUIRED DATA

Data taken on an Elekta Infinity at Mary Bird Perkins Cancer Center (Baton Rouge, LA) is presented in Fig. 7 for electron beams of nominal energies 10, 13 and 16 MeV.
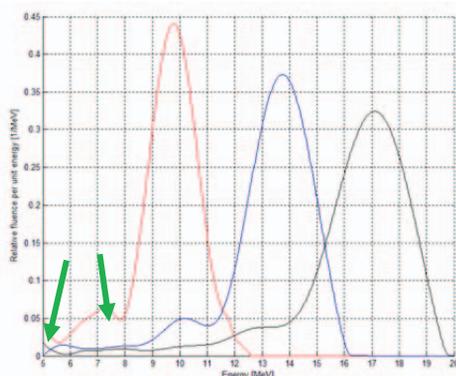

Figure 7: Measured electron energy spectra for an Elekta Infinity at nominal beam energies of 10, 13 and 16 MeV. The arrows note non-physical artifacts in the spectra.

Table 2 lists the spectral parameters calculated from the measured, unfolded spectra. When comparing the measured values in Table 2 to values measured with the previous, passive version of our spectrometer [5], the FWHM values were within 0.3 MeV, and the peak mean energies agreed within 0.6 MeV. Some of the unfolded spectra exhibit low energy upturn artifacts that were not present in the data from our passive spectrometer. The cause is being investigated, and is likely due to the unfolding process matching unsuppressed noise.

Table 2: Measured Energy Spectrum Parameters

	Peak Mean Energy Ep [MeV]	FWHM [MeV]
10 MeV	9.75	2.12
13 MeV	13.78	2.71
16 MeV	17.11	3.29

CONCLUSION AND FUTURE WORK

Our real-time spectrometer system allows for the real-time measurement of electron energy spectra. We are investigating the device's utility to assist in beam matching for medical linacs, as well as for routine quality assurance measurements such as energy constancy

We are currently analyzing the uncertainty associated with our measurements and spectral unfolding method. Ideally, to quantify any systemic error we would like to characterize our device with a mono-energetic beam that is itself accurately known. We are also investigating improvements to the method for unfolding the spectrum, such as using a different initial guess or using a weighting scheme.

REFERENCES

[1] ICRU, "Radiation Dosimetry: Electrons with Initial Energies Between 1 and 50 MeV", International Commision on Radiation Units and Measurements, Bethesda, MD 35, 1984.

[2] B. A. Faddegon and I. Blevis, "Electron spectra derived from depth dose distributions", *Med Phys,* vol. 27, pp. 514-26, Mar 2000.

[3] O. A. Ali, C. A. Willemse, W. Shaw, F. H. O'Reilly, and F. C. du Plessis, "Monte carlo electron source model validation for an Elekta Precise linac," *Med Phys,* vol. 38, pp. 2366-73, May 2011.

[4] J. G. Kok and J. Welleweerd, "Finding mechanisms responsible for the spectral distribution of electron beams produced by a linear accelerator", *Med Phys,* vol. 26, pp. 2589-96, Dec 1999.

[5] D. J. McLaughlin, K. R. Hogstrom, R. L. Carver, J. P. Gibbons, P. M. Shikhaliev, K. L. Matthews, *et al.*, "Permanent-magnet energy spectrometer for electron beams from radiotherapy accelerators", *Medical Physics,* vol. 42, pp. 5517-5529, 2015.

[6] C. Gahn, G. D. Tsakiris, K. J. Witte, P. Thirolf, and D. Habs, "A novel 45-channel electron spectrometer for high intensity laser-plasma interaction studies," *Review of Scientific Instruments,* vol. 71, p. 1642, 2000.